Microwave spectrum of toluene · SO_2: Structure, barrier to internal rotation, and dipole moment

Amine Taleb-Bendiab, Kurt W. Hillig II, and Robert L. Kuczkowski
Department of Chemistry, The University of Michigan, Ann Arbor, Michigan 48109-1055

(Received 9 October 1992; accepted 25 November 1992)

The microwave spectrum of toluene · SO_2 was observed with a pulsed beam Fourier-transform microwave spectrometer. The spectrum displays *a*-, *b*-, and *c*-dipole transitions. The transitions occur as doublets arising from the internal rotation of the methyl group. The transitions were assigned using the principal-axis method (PAM) internal rotation Hamiltonian with centrifugal distortions. Assuming a threefold symmetry for the internal rotation potential, the barrier height was determined as $V_3=83.236(2)$ cm^{-1}. The torsional–rotational spectra of toluene-CD_3 · SO_2 and toluene-d_8 · SO_2 were also assigned. Additional small splittings of the *c*-dipole transitions for the normal species and toluene-CD_3 · SO_2 suggest a reorientation tunneling motion of SO_2 with respect to the aromatic plane. The moment of inertia data show that the two monomer units are separated by $R_{cm}=3.370(1)$ Å, with the SO_2 located above the aromatic ring. The projection of the C_2 axis of SO_2 on the aromatic plane makes an angle of $\tau=47.0(1)°$ with the C_3 axis of toluene. The dipole moment of the complex is $\mu_T=1.869(27)$ D.

I. INTRODUCTION

The ability of sulfur dioxide to interact with the aromatic ring has long been noted.[1–4] Using spectrophotometric procedures, Andrews and Keefer investigated the complex between SO_2 and benzene and a series of methyl substituted benzene derivatives.[1] They suggested that the stability of the complexes increased with methyl substitution on the benzene ring. Apart from the fact that SO_2 interacts with the π system, detailed structural data from the above studies[1,4] as well as more recent matrix infrared (IR) studies[5] are generally lacking. We recently reported the microwave spectrum of benzene · SO_2, and showed that SO_2 is located above the benzene ring with the sulfur end tilted towards the π system.[6,7] These studies motivated us to investigate the microwave spectrum of toluene · SO_2 to determine the effect of methyl group substitution on the conformation and the stability of the complex.

We were also interested in the effect of complexation on possible internal motions. Rudolph *et al.* showed that the methyl group in toluene exhibits nearly free internal rotation about its symmetry axis with a barrier $V_6=4.9$ cm^{-1}.[8] Moreover, we found in benzene · SO_2 (Ref. 7) that the benzene ring is almost freely rotating about its C_6 axis with a barrier $V_6=0.28$ cm^{-1}. Consequently, the prospect of studying such motions in toluene · SO_2 was attractive.

II. EXPERIMENT

The microwave spectrum of toluene · SO_2 was observed in a Balle–Flygare Fourier-transform microwave (FTMW) spectrometer with a pulsed nozzle source.[9] A mixture of ~1% C_7H_8, 1% SO_2, and 98% Ne maintained at a pressure of 1–2 atm was employed to generate the spectrum. The transitions had full-widths at half-maximum of ~15–30 kHz and the frequency measurement accuracy is estimated to be 4 kHz (unless otherwise stated).

For the measurement of Stark effects, the spectrometer was equipped with steel mesh plates separated by 30 cm to which up to 10 kV can be applied with opposite polarities.[10] The $2_{02}\leftarrow1_{11}$ transition of SO_2 was used as an electric field calibration standard [$\mu(SO_2)=1.633\,05$ D (Ref. 11)].

The spectra of the isotopically substituted species were observed in enriched samples. Toluene-CD_3 (98% enrichment, Cambridge Isotope Laboratories) and toluene-d_8 (99% enrichment, Aldrich Chemical Co.) were used without dilution. $S^{18}O_2$ (99% enrichment, Alfa Products) was used without dilution to assign the toluene · $S^{18}O_2$ spectrum. The spectra of toluene · $S^{16}O^{18}O$ species were observed starting with a 50%–50% mixture of $S^{16}O_2$ and $S^{18}O_2$, which equilibrates in our glass sample bulbs to form a statistical 2:1:1 mixture of $S^{16}O^{18}O$:$S^{16}O_2$:$S^{18}O_2$.

III. RESULTS AND ANALYSIS

A. Spectral assignments

In the work reporting the microwave spectrum of benzene · SO_2 we showed that the two subunits are stacked one above the other and their centers-of-mass are separated by ~3.48 Å.[6,7] Based on their ultraviolet (UV) studies, Andrews and Keefer also claimed that the SO_2 complexes of benzene, and several of its derivatives, including toluene, are closely similar.[1] In light of these results, the assumption of a similar conformation for toluene · SO_2 to that of benzene · SO_2 was a reasonable starting point for spectral analysis. The initial frequency regions we searched were based on a structure where the SO_2 molecular plane and the aromatic ring were parallel and separated by a distance of 3.48 Å. Moreover, toluene is known to undergo a nearly free methyl torsion internal rotation.[8] If this internal motion is not quenched upon complexation, the spectrum of toluene · SO_2 would be complicated by the presence of additional transitions.

 0021-9606/93/053627-10$06.00

TABLE I. Ground torsional state ($m=0$) spectroscopic constants of toluene · SO_2.[a]

	$C_6H_5CH_3 \cdot SO_2$	$C_6H_5CD_3 \cdot SO_2$	$C_6D_5CD_3 \cdot SO_2$	$C_6H_5CH_3 \cdot S^{18}O_2$	$C_6H_5CH_3 \cdot S^{18}OO$	$C_6H_5CH_3 \cdot SO^{18}O$
A' /MHz	1499.175(2)[b]	1394.286(2)	1275.468(5)	1473.037(4)	1488.335(8)	1485.048(6)
B' /MHz	933.9663(2)	919.7895(3)	875.9449(10)	900.0356(4)	912.8626(16)	919.7877(6)
C' /MHz	749.1058(2)	718.1812(2)	692.1163(5)	723.4529(3)	734.5433(5)	737.3651(4)
D_J /kHz	0.421(3)	0.368(5)	0.325(7)	0.410(3)	0.409(10)	0.414(7)
D_{JK} /kHz	3.32(3)	3.19(3)	2.58(7)	3.00(3)	3.42(27)	2.96(4)
D_K /kHz	−3.6(4)	−3.4(4)	−2.8(5)	−3.7(6)	···	−3.2(10)
d_1 /kHz	−0.070(1)	−0.070(2)	−0.060(4)	−0.062(2)	−0.076(7)	−0.063(3)
d_2 /kHz	−0.078(2)	−0.084(2)	−0.069(3)	−0.071(2)	−0.088(8)	−0.070(3)
n[c]	28	25	18	21	12	19
$\Delta\nu_{rms}$[d] /kHz	2	2	3	2	2	2

[a]The spectroscopic constants are determined using Watson S-reduced semirigid-rotor Hamiltonian in I^r representation (Ref. 12).
[b]The uncertainties are 1σ.
[c]Number of transitions.
[d]$\Delta\nu=\nu_{obs}-\nu_{calc}$.

The $J=5\leftarrow4$ rigid-rotor a-dipole transitions for toluene · SO_2 were predicted to occur in the region between 8–9 GHz and after searching a portion of this region, we observed several transitions. From qualitative Stark effect measurements, we classified these transitions into two groups. One group corresponded to transitions with a second-order Stark effect, and the second group of transitions displayed a first-order Stark effect. The existence of first-order Stark effect transitions in the spectrum implied the existence of degenerate energy levels. These observations suggested that the internal rotation of the methyl group was indeed perturbing the spectrum of toluene · SO_2, and that, the two groups of transitions correspond to $m=0$ and ±1 states (designated A and E, respectively), where m is the internal rotation quantum number.

1. Ground torsional state ($m=0$)

In the first stage of the spectral analysis, we focused on the assignment of the ground torsional state ($m=0$) transitions. In the ground torsional state the transitions would follow a semirigid-rotor pattern (no quantum of internal rotational angular momentum). In fact this is true only if the torsional motion is the sole tunneling present in the complex, otherwise the transitions will be further perturbed, especially for the case of an inversionlike tunneling motion. Several transitions were assigned to the R-branch a-dipole spectrum and were fit with a semirigid-rotor Hamiltonian. Fitting the a-type transitions led to very accurately determined rotational constants. The asymmetry factor κ was equal to -0.5, indicating that toluene · SO_2 is quite asymmetric. Since the rotational constants are well determined from the a-type spectrum, the b- and c-type spectra could be accurately predicted. Using this prediction, four b-dipole and three c-dipole transitions were then observed. The b-dipole transitions were found a few kHz from their respective predictions. However, the c-dipole transitions were found as doublets split ~50 kHz to either side of the predictions. The occurrence of doublets will be discussed later in this section, however in the fitting analyses only their corresponding averaged frequencies were used. The rotational constants A', B', and C', and five quartic centrifugal distortion constants D_J, D_{JK}, D_K, d_1, and d_2 were derived from a least-squares fit of a total of 28 A state ($m=0$) transitions. These spectroscopic constants which were derived using the Watson S-reduction Hamiltonian[12] (I^r representation) are listed in Table I. The A state transitions are listed in Table II under the $m=0$ column. The fit of these transitions was also undertaken using the A-reduction quartic centrifugal distortion constants Δ_J, Δ_{JK}, Δ_K, δ_J, and δ_K since these parameters might be more

TABLE II. Torsional-rotational transitions of $C_6H_5CH_3 \cdot SO_2$.

	A $m=0$		E $m=\pm1$	
$J'_{K'_aK'_c}-J''_{K''_aK''_c}$	ν_{obs}(MHz)	$\Delta\nu$(kHz)[a]	ν_{obs}(MHz)	$\Delta\nu$(kHz)[a]
$5_{05}-4_{04}$	7 902.261	4	7 871.113	8
$5_{15}-4_{14}$	7 828.834	4	7 869.786	−1
$5_{14}-4_{13}$	8 655.532	3	8 460.906	−23
$5_{24}-4_{23}$	8 330.019	3	8 280.093	−1
$5_{23}-4_{22}$	8 838.411	1	8 790.547	3
$5_{33}-4_{32}$	8 502.322	−4	8 538.853	1
$5_{32}-4_{31}$	8 599.800	−2	8 626.828	−1
$6_{06}-5_{05}$	9 383.241	1	9 340.541	9
$6_{16}-5_{15}$	9 345.147	2	9 400.333	−9
$6_{15}-5_{14}$	10 224.932	−1	10 129.785	−13
$6_{25}-5_{24}$	9 930.118	−0	9 883.321	8
$6_{24}-5_{23}$	10 625.616	1	10 408.020	1
$6_{34}-5_{33}$	10 198.331	−2	10 194.240	−4
$6_{33}-5_{32}$	10 427.033	−1	10 506.471	1
$7_{07}-6_{06}$	10 870.368	−1	10 826.865	11
$7_{17}-6_{16}$	10 852.488	3	10 903.357	−22
$7_{16}-6_{15}$	11 724.960	−6	11 710.856	−11
$7_{26}-6_{25}$	11 501.930	−2	11 483.734	25
$7_{25}-6_{24}$	12 352.094	−4	12 036.837	10
$7_{35}-6_{34}$	11 874.415	−6	11 828.890	5
$7_{34}-6_{33}$	12 292.812	3	12 342.306	−1
$6_{16}-5_{05}$	9 414.589	1		
$6_{06}-5_{15}$	9 313.802	5		
$7_{17}-6_{06}$	10 883.831	−2		
$7_{07}-6_{16}$	10 839.021	1		
$4_{13}-3_{03}$	8 375.535[b]	4 ($\Delta=111$)[c]		
$5_{14}-4_{04}$	10 612.040[b]	1 ($\Delta=115$)[c]		
$6_{15}-5_{05}$	12 934.717[b]	2 ($\Delta=97$)[c]		

[a]$\Delta\nu=\nu_{obs}-\nu_{calc}$ using the constants in Table V.
[b]The uncertainties are estimated to be 10 kHz.
[c]Δ is the splitting (in kHz) between the c-type frequency doublets.

TABLE III. Torsional-rotational transitions (in MHz) for the deuterated isotopic species of toluene · SO_2.

	$C_6H_5CD_3 \cdot SO_2$				$C_6D_5CD_3 \cdot SO_2$			
	A $m=0$		E $m=\pm1$		A $m=0$		E $m=\pm1$	
$J'_{K'_aK'_c}-J''_{K''_aK''_c}$	ν_{obs}	$\Delta\nu$[a]	ν_{obs}	$\Delta\nu$[a]	ν_{obs}	$\Delta\nu$[a]	ν_{obs}	$\Delta\nu$[a]
$5_{05}-4_{04}$	7 578.329	−1	7 568.753	−1				
$5_{15}-4_{14}$	7 528.827	1	7 536.920	1				
$5_{14}-4_{13}$	8 381.073	1	8 371.541	2				
$5_{24}-4_{23}$	8 075.089	−0	8 069.009	1				
$5_{23}-4_{22}$	8 677.088	−0	8 662.679	−1				
$5_{33}-4_{32}$	8 296.205	−0						
$5_{32}-4_{31}$	8 451.781	−1						
$6_{06}-5_{05}$	9 000.204	−1	8 987.342	−1	8 642.430	−1	8 630.477	3
$6_{16}-5_{15}$	8 978.296	2	8 989.401	−2	8 626.256	1	8 636.697	−1
$6_{15}-5_{14}$	9 846.135	2	9 843.010	1	9 390.970	−0	9 388.647	−1
$6_{25}-5_{24}$	9 604.269	−2	9 599.452	−1	9 192.663	−4	9 189.068	2
$6_{24}-5_{23}$	10 392.072	1	10 368.715	−0	9 915.096	−1	9 892.151	−1
$6_{34}-5_{33}$	9 938.566	1	9 929.956	−1	9 508.695	−2	9 501.351	1
$6_{33}-5_{32}$	10 278.806	1	10 272.396	0	9 845.138	3	9 839.052	1
$7_{07}-6_{06}$	10 429.114	0	10 418.446	2	10 020.917	−2	10 011.417	1
$7_{17}-6_{16}$	10 420.266	0	10 428.943	−3	10 014.692	1	10 022.452	−4
$7_{16}-6_{15}$	11 253.952	−2	11 250.415	−1	10 744.714	2	10 739.938	−2
$7_{26}-6_{25}$	11 100.841	−1	11 099.818	3	10 626.447	−0	10 627.729	2
$7_{25}-6_{24}$	12 018.299	−0	11 996.990	−1	11 453.716	2	11 435.282	2
$7_{35}-6_{34}$			11 540.068	3	11 046.298	−1	11 037.552	0
$7_{34}-6_{33}$			12 105.631	−1	11 593.893	−1	11 578.968	−3
$6_{16}-5_{05}$	9 014.327	−2						
$6_{06}-5_{15}$	8 964.167	−3						
$7_{17}-6_{06}$	10 434.393	4			10 024.385	6		
$7_{07}-6_{16}$	10 414.989	−1			10 011.229	−2		
$8_{18}-7_{07}$					11 403.770	−0		
$8_{08}-7_{17}$					11 399.115	−1		
$5_{14}-4_{04}$	10 424.471[b]	1 ($\Delta=75$)[c]						
$6_{15}-5_{05}$	12 692.271[b]	−2 ($\Delta=57$)[c]						

[a]See footnote a in Table II.
[b]See footnote b in Table II.
[c]See footnote c in Table II.

appropriate for very asymmetric rotors. The root-mean-square (rms) of the fit was identical to that obtained from the S-reduction and equal to 2 kHz. In addition, when both sets of quartic centrifugal distortion constants were transformed into τ's,[12] they led to identical values within uncertainty limits. Throughout the remainder of this section the S-reduction parameters will be used.

The $m=0$ spectra of toluene-$CD_3 \cdot SO_2$, toluene-$d_8 \cdot SO_2$, toluene · $S^{18}O_2$, and two different toluene · $S^{18}OO$ isotopic species were also assigned. The transitions for the deuterated species are given in Table III under the $m=0$ columns, and those for the ^{18}O species are listed in Table IV. The spectroscopic constants obtained using the Watson Hamiltonian (see above) are given in Table I. For the deuterated species no splittings nor broadening of the transitions were observed due to the deuterium nuclear quadrupole moment. For these two species the $m=\pm1$ spectra were also measured, and they will be considered in the internal rotation section. For the single-^{18}O and double-^{18}O species, no attempt was made to measure the b- and c-type transitions since the rotational constants were fairly well determined for reasons explained above. Furthermore, two $m=0$ spectra of single-^{18}O species were assigned, implying the existence of two nonequivalent oxygens.

2. Torsional-rotational spectrum ($m=0$ and ±1)

Apart from deducing the J quantum number from Stark effect measurements,[13] pairing the transitions arising from the E state ($m=\pm1$) with their counterparts from the A state ($m=0$) was not straightforward. This implies that the barrier to internal rotation of the methyl group is relatively low causing larger separations between transition doublets. Furthermore, for degenerate torsional spectra, and unlike the ground torsional state, the nonvanishing coupling terms between the overall rotation and the internal rotation (see below) can further perturb the E state spectrum.[14]

TABLE IV. The $m=0$ state rotational transitions (in MHz) for the ^{18}O isotopic species of toluene · SO_2.

	$C_6H_5CH_3 \cdot S^{18}O_2$		$C_6H_5CH_3 \cdot S^{18}OO$		$C_6H_5CH_3 \cdot SO^{18}O$	
$J'_{K'_aK'_c}-J''_{K''_aK''_c}$	ν_{obs}	$\Delta\nu^a$	ν_{obs}	$\Delta\nu^a$	ν_{obs}	$\Delta\nu^a$
$5_{05}-4_{04}$	7 638.810	0	7 752.600	0	7 782.066	1
$5_{15}-4_{14}$	7 561.379	1	7 675.104	−0	7 707.952	−1
$5_{14}-4_{13}$	8 359.284	1			8 525.715	2
$5_{24}-4_{23}$	8 039.855	−0	8 158.306	0	8 202.485	3
$5_{23}-4_{22}$	8 514.590	−0	8 638.734	−1	8 701.691	−2
$5_{33}-4_{32}$	8 198.089	1			8 371.045	−1
$5_{32}-4_{31}$	8 282.988	−3			8 465.286	3
$6_{06}-5_{05}$	9 068.674	−1	9 204.524	−3	9 239.645	−1
$6_{16}-5_{15}$	9 027.077	−1	9 163.031	3	9 200.891	−1
$6_{15}-5_{14}$	9 884.245	−1	10 027.071	0	10 073.032	−3
$6_{25}-5_{24}$	9 587.558	−0	9 728.857	−1	9 778.571	−1
$6_{24}-5_{23}$	10 243.540	0	10 392.086	0	10 463.042	−0
$6_{34}-5_{33}$	9 835.349	−1			10 041.311	−0
$6_{33}-5_{32}$	10 037.144	3			10 263.074	−2
$7_{07}-6_{06}$	10 503.970	3	10 661.985	2	10 703.207	2
$7_{17}-6_{16}$	10 483.781	−2	10 641.905	−3	10 684.874	−1
$7_{16}-6_{15}$	11 341.422	0	11 505.696	0	11 551.472	−1
$7_{26}-6_{25}$	11 108.810	−1			11 326.875	1
$7_{25}-6_{24}$	11 918.644	−0			12 165.446	2
$7_{35}-6_{34}$	11 455.306	1				
$7_{34}-6_{33}$	11 831.264	−1				

$^a\Delta\nu=\nu_{obs}-\nu_{calc}$ in kHz.

To predict the torsional-rotational spectrum of toluene · SO_2, we employed the PAM internal rotation Hamiltonian written as follows:[15]

$$\mathscr{H}=AP_a^2+BP_b^2+CP_c^2+\tfrac{1}{2}\sum_{i\neq j=a,b,c}D_{ij}(P_iP_j+P_jP_i)$$

$$-2\sum_{i=a,b,c}Q_iP_ip+Fp^2+\tfrac{1}{2}V_3(1-\cos 3\alpha), \qquad (1)$$

where

$$A=A_r+F\rho_a^2,\ B=B_r+F\rho_b^2,\ C=C_r+F\rho_c^2,$$

$$D_{ij}=F\rho_i\rho_j\ (i,j=a,b,c \text{ and } i\neq j),$$

$$Q_i=F\rho_i\ (i=a,b,c),$$

$$F=F_\alpha[1-\rho_a\cos(\theta_a)-\rho_b\cos(\theta_b)-\rho_c\cos(\theta_c)]^{-1},$$

$$\rho_a=\frac{A_r}{F_\alpha}\cos(\theta_a),\ \rho_b=\frac{B_r}{F_\alpha}\cos(\theta_b),\ \rho_c=\frac{C_r}{F_\alpha}\cos(\theta_c).$$

Several terms in this Hamiltonian have been defined in the work on benzene · SO_2.[7] Since a-, b-, and c-dipole transitions occur in the $m=0$ spectrum, none of the three direction cosines with respect to the principal axes necessarily vanish. Therefore in the above Hamiltonian, and unlike in the benzene · SO_2 case,[7] terms that are dependent on the θ_b angle are also present. Since in toluene · SO_2 the methyl group is the internal rotor, a threefold barrier is used where V_3 is the barrier height. The Hamiltonian matrix of $\mathscr{H}$ is constructed with the usual basis set, that is, $|JKM\rangle\cdot|m\rangle$. The infinite Hamiltonian matrix, factored into A and E sub-blocks, is truncated at a given m value when an acceptable energy convergence is attained.

Using the above Hamiltonian [Eq. (1)] we made predictions of the E state spectrum by increasing the barrier height V_3 by increments of 5–10 cm^{-1} starting from the free rotor case. While we varied the barrier, we maintained the rigid-rotor constants fixed at the A state values (see Table I). We also set the internal rotor axis collinear to the b-axis of the complex which is in agreement with a qualitative analysis of the observed A state rotational constants. For a barrier height around 85 cm^{-1} several E state transitions were matched with the prediction. To confirm the assignment, additional transitions were measured from the predictions for this barrier height.

The fit of the torsional-rotational spectrum ($m=0$ and ±1) of toluene · SO_2 was undertaken using the PAM internal rotation Hamiltonian in Eq. (1). To account for centrifugal distortion effects, the following expression was added:

$$\mathscr{H}_{dist.}=-D_JP^4-D_{JK}P^2P_a^2-D_KP_a^4+d_1P^2(P_+^2+P_-^2)$$
$$+d_2(P_+^4+P_-^4)-D_{Jm}P^2p^2-D_{Km}P_a^2p^2$$
$$+d_mp^2(P_+^2+P_-^2)+2L_{Ja}P^2P_ap+2L_{Jb}P^2P_bp, \qquad (2)$$

where $P_\pm=P_b\pm iP_c$. Besides the first five terms in Eq. (2) (Watson S-reduction quartic Hamiltonian[12]), the remaining ones were added empirically employing the standard Hamiltonian similar to that introduced by Rohart.[16]

The Hamiltonian matrix, factored into A and E sub-blocks, was diagonalized with the free rotor basis set truncated at $m=\pm14$. The moment of inertia I_α [inversely proportional to F_α in Eq. (1)] of the internal rotor about the C_3 axis was fixed at the value 3.14 amu Å^2 determined

TABLE V. Spectroscopic constants for toluene · SO_2 derived using the internal rotation Hamiltonian.

	$C_6H_5CH_3 \cdot SO_2$	$C_6H_5CD_3 \cdot SO_2$	$C_6D_5CD_3 \cdot SO_2$
A /MHz	1499.30(4)[a]	1394.34(2)	1275.56(3)
B /MHz	936.815(3)	928.762(3)	883.984(5)
C /MHz	749.117(2)	718.239(2)	692.171(3)
D_J /kHz	0.411(14)	0.368(4)	0.328(6)
D_{JK} /kHz	3.20(9)	3.20(3)	2.62(6)
D_K /kHz	−4.5(16)	−3.4(3)	−3.1(5)
d_1 /kHz	−0.064(7)	−0.071(2)	−0.063(3)
d_2 /kHz	−0.074(5)	−0.086(2)	−0.072(3)
D_{Jm} /kHz	−188.7(5)	−130.3(4)	−127.0(6)
D_{Km} /kHz	220.0(208)	135.7(56)	124.1(85)
d_m /kHz	83.2(5)	60.3(3)	58.1(5)
L_{Ja} /kHz	7.4(13)	⋯	⋯
L_{Jb} /kHz	−2.7(8)	⋯	⋯
V_3 /cm^{-1}	83.236(2)	84.160(2)	84.352(3)
θ_a /deg.	85.133(1)	87.976(6)	85.844(7)
θ_b /deg.	10.012(1)	7.502(2)	8.541(2)
n[b]	49	44	32
$\Delta\nu_{rms}$[c] /kHz	9	2	3
A_r[d] /MHz	1499.197	1394.306	1275.449
B_r /MHz	931.439	918.113	874.379
C_r /MHz	749.035	718.135	692.067
Q_a /MHz	127.957	49.812	93.463
Q_b /MHz	922.713	920.966	874.383
Q_c /MHz	114.337	91.324	90.729
D_{ab} /MHz	0.746	0.576	1.027
D_{bc} /MHz	0.666	1.056	0.997
D_{ac} /MHz	0.092	0.057	0.107
F /MHz	158 375.824	79 645.799	79 602.699
θ_c /deg.	81.272	82.779	82.551

[a]The uncertainties are 1σ.
[b]Number of transitions.
[c]$\Delta\nu = \nu_{obs} - \nu_{calc}$.
[d]A_r, B_r, C_r, Q_i, D_{ij} (i, j=a, b, or c) and F are derived from the fitted parameters using the relationships in Eq. (1).

from the structure of free toluene.[17] The fit of the $m=0$ and ± 1 transitions for toluene · SO_2 normal species is given in Table II. Examination of the splitting between each torsional doublet in Table II, shows that the frequency separation varies from 30 to 195 MHz for the a-type transitions. The derived spectroscopic constants are listed in Table V. The angles θ_a and θ_b between the internal rotor axis and the a and b axes, respectively, were derived from the fit. However, θ_c was adjusted internally after each fitting iteration using the squared cosine relationship $[\cos^2(\theta_a)+\cos^2(\theta_b)+\cos^2(\theta_c)=1]$. In fact an attempt to fit the three angles simultaneously was undertaken while the cosine relationship constraint was relaxed, but the angles were very strongly correlated. The values of the angles θ_a, θ_b, and θ_c (see Table V) indicate that the internal rotor axis is nearly aligned with the b axis of the complex. Including the terms with constants D_{Jm}, D_{Km}, d_m, L_{Ja}, and L_{Jb} relevant to internal rotation, has improved the quality of the fit greatly with the rms deviation of the fit decreased from 600 to 9 kHz. In fact these additional terms were also useful in choosing the right assignment for some E state transitions for the normal species such as $5_{05} \leftarrow 4_{04}$ and $5_{15} \leftarrow 4_{14}$ which were separated by $\sim$1.5 MHz (see Table II). Like in the work on benzene · SO_2,[7] the parameters A_r, B_r, C_r, Q_i, D_{ij} ($i,j=a$, b or c) and F are adjusted internally after each iteration based on the expressions [see Eq. (1)] relating them to the fitted parameters. The angle θ_c was determined as explained above. The barrier height V_3 was also derived, and it is given in Table V. Attempts to measure transitions from $m=\pm 2$ states and higher were not made since these levels tend to be placed very high compared to the first two torsional levels $m=0$ and ± 1 when internal rotation involves a very light top such as a methyl group. In fact the separation between the $m=\pm 1$ and ± 2 states is $\sim$40 cm^{-1} for the normal species, and these higher levels ($m \geqslant \pm 2$) are not populated due to the low temperature of the molecular beam ($\sim$2 K).

As mentioned above, we also investigated the torsional-rotational spectra of toluene-CD_3 · SO_2 and toluene-d_8 · SO_2. The prediction and assignment of the $m=\pm 1$ transitions of these two deuterated species was accomplished using the barrier height determined for the normal species. The PAM internal rotation Hamiltonian [Eq. (1)] and the distortion terms [Eq. (2)] were also employed for these two isotopic species; the Hamiltonian matrix setup discussed for the normal species is identical for these isotopic species. The matrix was again truncated at $m=\pm 14$. The internal rotor moment of inertia I_α was fixed at 6.21 amu Å^2 for a deuterated methyl group.[17] The least-squares fits of transitions for both A and E torsional states for toluene-CD_3 · SO_2 and toluene-d_8 · SO_2 are given in Table III. The corresponding spectroscopic constants obtained from the fit are listed in Table V. Discussions about the fitted parameters and nonfitted parameters made for the normal species apply to these two deuterated species as well. The constants L_{Ja} and L_{Jb}, which are undetermined for toluene-CD_3 · SO_2 and toluene-d_8 · SO_2, were set equal to zero.

3. Origin of the splitting in the c-dipole transitions

For the normal species and also toluene-CD_3 · SO_2, a small splitting of $\sim$100 kHz was observed in the A state, c-dipole transitions (see Tables II and III); however, no such splitting was observed in the a- and b-type transitions. These observations suggest that in addition to the methyl group internal rotation, the complex is exhibiting a high barrier tunneling motion accompanied by a change of direction of the dipole moment of the complex along the c axis ($\mu_c \leftrightarrow -\mu_c$). Based on these observations and structural inferences discussed below, two possible tunneling pathways can be considered. Starting with reference conformation 1 in Fig. 1, the first pathway $1 \rightarrow 2$ corresponds to a rotation of SO_2 about its $SO_{(a)}$ bond followed by a readjustment of its molecular plane as well as a readjustment of the aromatic plane depending on the detailed structure (see Sec. III C). The second pathway $1 \rightarrow 3$ is equivalent to a rotation of the SO_2 molecular plane about the aromatic ring by 120° clockwise (or 240° counterclockwise) plus other angular readjustments depending on the detailed structure of the complex. Selecting the pathway that leads to the observable splitting for toluene · SO_2 is, however, impossible due to a lack of experimental data. Nevertheless, results from the torsional-rotational analyses

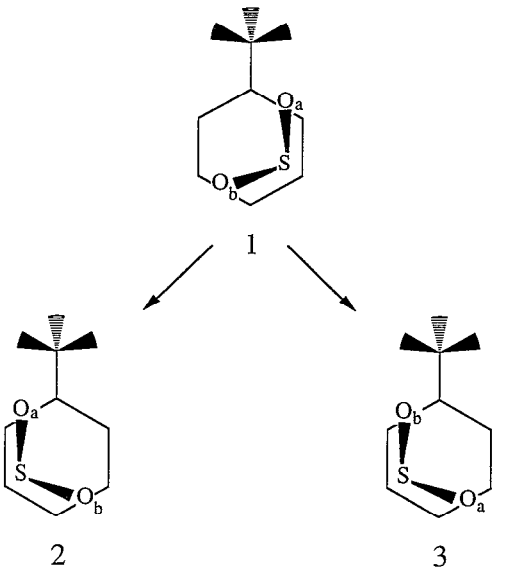

FIG. 1. The two possible reorientation pathways 1→2 and 1→3 causing splittings in the *c*-type transitions of toluene · SO_2.

for toluene · SO_2 will not be affected since this reorientation tunneling motion is a small perturbation on the spectra. Similar reorientation tunneling motion effects were also observed in the microwave spectrum of furan · SO_2 (Ref. 18) which has a similar structure. The possibility of SO_2 rotating about its C_2 axis cannot account for the splitting in the *c*-type transitions since the permutation of oxygens (spin zero) would only lead to one level with nonzero spin weight.

B. Dipole moment

Since the ground torsional state ($m=0$) spectrum of toluene · SO_2 is that of a semirigid-rotor, Stark effect coefficients may be calculated by a second-order perturbation treatment.[13] To calculate these coefficients, the effective rotational constants for the normal species listed in Table I were employed. As discussed for benzene · SO_2 (Refs. 7 and 19), the dipole moment components will be those along the effective principal axes, which differ from the actual principal axes. However, an inspection of the effective rotational constants in Table I and the rigid-rotor rotational constants A_r, B_r, and C_r in Table V for the normal species, suggests that the difference is quite negligible.

The Stark shifts for twelve M components from four transitions, arising from the ground torsional state ($m=0$), were measured. The second-order Stark coefficients were obtained from fits of $\Delta\nu$ vs $\mathscr{E}^2$. The observed coefficients are listed in Table VI. A least-squares fit of the observed coefficients yielded a total dipole moment, $\mu_T=1.869(27)$ D, with components $\mu_a=1.640(29)$ D, $\mu_b=0.283(52)$ D, and $\mu_c=0.852(4)$ D.

TABLE VI. Stark coefficients for the ground torsional state ($m=0$) transitions and dipole moment of toluene · SO_2.

Transition	$\lvert M\rvert$	$\Delta\nu/\mathscr{E}^2$ [a]	obs−calc
5_{05}–4_{04}	0	−0.163	−0.004
	1	−2.249	0.025
5_{15}–4_{14}	0	−0.122	−0.003
	1	2.206	0.022
5_{14}–4_{13}	0	−0.147	0.004
	1	−0.207	0.002
	2	−0.388	−0.006
	3	−0.674	−0.006
	4	−1.068	0.003
6_{15}–5_{14}	2	−0.471	−0.013
	3	−0.928	−0.004
	4	−1.574	0.003
		$\lvert\mu_a\rvert=1.640(29)$ [b] D	
		$\lvert\mu_b\rvert=0.283(52)$ D	
		$\lvert\mu_c\rvert=0.852(4)$ D	
		$\lvert\mu_T\rvert=1.869(27)$ D	

[a] Observed Stark coefficients in units of 10^{-5} MHz/(V/cm)^2.
[b] The uncertainties are 2σ.

C. Structure

The planar moments of inertia for the normal species of toluene · SO_2 are $P_{aa}=1/2(I_b+I_c-I_a)=\Sigma m_i a_i^2$ =439.32 amu Å^2, $P_{bb}=235.32$ amu Å^2, and $P_{cc}=101.79$ amu Å^2. These values were determined using the constants in Table I which are in fact contaminated by the internal rotation. However, the small difference between these constants and the rigid-rotor constants (see Table V), makes their use justified. Effective rotational constants for all species in Table I will be used throughout the structural analysis.

The successful prediction of the $m=0$ state spectrum was a result of using a structural model where SO_2 is located on top of the aromatic ring (see Sec. III A). Starting from this conformation with the C_2 axis of SO_2 parallel to the C_3 axis of toluene, the predicted P_{bb} and P_{cc} are

$$P_{bb}(\tau=0^\circ \text{ or } 180^\circ)=P_{bb}(SO_2)+P_{aa}(\text{toluene}) =209.20 \text{ amu Å}^2, \quad (3)$$

and

$$P_{cc}(\tau=0^\circ \text{ or } 180^\circ)=P_{aa}(SO_2)+P_{bb}(\text{toluene}) =137.29 \text{ amu Å}^2, \quad (4)$$

where the values of $P_{aa}(SO_2)$ and $P_{bb}(SO_2)$, and P_{aa}(toluene) and P_{bb}(toluene) are 49.05 and 8.38 amu Å^2,[20] and 200.82 and 88.24 amu Å^2,[17,21] respectively. Equations (3) and (4) are obtained assuming that the SO_2 molecular plane and the aromatic plane are parallel, and separated by a fixed distance which does not affect the values of P_{bb} and P_{cc}. The parameter τ is the torsional angle between the projection of the C_2 axis on the aromatic plane and the C_3 axis. The configuration where the sulfur atom is closest to the *para* position with the C_2 and C_3 axes parallel is chosen, arbitrarily, as $\tau=0^\circ$. The fact that the observed and predicted P_{bb} and P_{cc} (see above) for toluene · SO_2 normal species are not in good agreement is a clear indication that τ is different from 0° or 180°, which implies that the complex has no plane of symmetry in its equilibrium configuration. This is supported by the observation of *a*-, *b*-, and

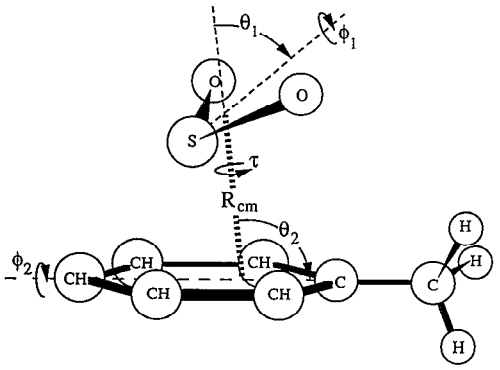

FIG. 2. The six structural parameters which define the geometry of toluene · SO_2.

TABLE VIII. Observed dipole moment components and Kraitchman substitution coordinates for the two oxygens compared with values calculated for structures I and II from Table VII.

	Obs	I	II
$\lvert\mu_a\rvert$ /D	1.640	1.053	1.080
$\lvert\mu_b\rvert$ /D	0.283	0.333	1.076
$\lvert\mu_c\rvert$ /D	0.852	0.944	1.033
$\lvert a(O_1)\rvert$ /Å	1.988	2.007	2.024
$\lvert b(O_1)\rvert$ /Å	1.211	1.219	1.310
$\lvert c(O_1)\rvert$ /Å	0.461	0.443	0.279
$\lvert a(O_2)\rvert$ /Å	2.420	2.440	2.437
$\lvert b(O_2)\rvert$ /Å	0.939	0.968	0.860
$\lvert c(O_2)\rvert$ /Å	0.648	0.621	0.828

c-dipole transitions. The assignment of two different spectra for the single-^{18}O species is also consistent with the nonexistence of a plane of symmetry.

In addition to the torsional angle τ, there are five other structural parameters that describe the relative orientation between the two subunits assuming that the geometries of toluene and SO_2 are unchanged upon complexation.[17,22] These five parameters are the distance R_{cm} between the centers-of-mass of toluene and SO_2; the tilt angle θ_1 between R_{cm} and the C_2 axis of SO_2; the twist angle ϕ_1 between R_{cm} and the molecular plane of SO_2; the tilt angle θ_2 between R_{cm} and C_3 axis of toluene; and the twist angle ϕ_2 between R_{cm} and the aromatic plane (methyl is held fixed rigidly to the aromatic ring). All six structural parameters are shown in Fig. 2. The conformations where the molecular plane of each subunit is perpendicular to R_{cm} correspond to ϕ_1 and ϕ_2 each equal to 90°. The six structural parameters were determined by a least-squares fit of the moments of inertia of all the isotopic species. Since in the above analysis of the planar moments, P_{bb} and P_{cc} of toluene · SO_2 are identical for $\tau=0°$ or 180°, two structure candidates are likely, depending on the initial choice of the torsional angle orientation. Hence, two least-squares fits were performed corresponding to conformations starting with τ at 60° and then 120°. The two fits labeled I and II, respectively, yielded the six structural parameters listed in Table VII. The main difference between the two conformations is in the torsional angle τ, and an appropriate readjustment of the two twist angles ϕ_1 and ϕ_2. Elimination of either conformation based on the standard deviation of the fit ΔI_{rms} (where, $\Delta I=I_{obs}-I_{calc}$) was not possible because of the reasonable quality of the fit for both cases (see Table VII). The tilt angles θ_a, θ_b, and θ_c between the axis of internal rotation (C_3 axis) and the principal axes a, b, and c, respectively, were calculated from each fit. For the normal species these values were $\theta_a=85.58°$, $\theta_b=10.04°$, and $\theta_c=81.01°$ for fit I, and $\theta_a=86.09°$, $\theta_b=10.06°$, and $\theta_c=80.75°$ for fit II. These values are in very good agreement with those derived directly from the internal rotation fit in Table V. These angles were also calculated for the two deuterated isotopic species and are in good agreement as well.

TABLE VII. Structural parameters for toluene · SO_2 from least-squares fits using the rotational constants of all isotopic species in Table I.

	I[a]	II
R_{cm} /Å	3.370(1)[b]	3.369(1)
τ /deg	47.0(1)	134.8(24)
θ_1 /deg	52.2(42)	44.8(69)
ϕ_1 /deg	101.6(14)	77.7(29)
θ_2 /deg	87.0(6)	88.3(10)
ϕ_2 /deg	80.6(8)	100.7(14)
ΔI_{rms} /amu Å^2[c]	0.21	0.38

[a]Preferred fit (see text).
[b]The uncertainties are 2σ.
[c]$\Delta I=I_{obs}-I_{calc}$.

A choice between the two possibilities can be made by comparing the dipole components and the values of the oxygen coordinates predicted from each conformation with the observed dipole components and the Kraitchman substitution coordinates[23] obtained from the single-^{18}O data. The predicted dipole components were obtained from a vector sum of the dipole moments of the two subunits, $\mu(SO_2)=1.633\,05$ D (Ref. 11) and $\mu(\text{toluene})=0.375$ D.[8] The predicted and observed values are given in Table VIII. The large value for μ_b predicted for the conformation from fit II is not observed, which makes this structure unlikely. The large difference between μ_a from the vector sum for both fits and that determined experimentally can be attributed mostly to the induced dipole moment arising from the large polarization of the π system of toluene. However, it is unlikely that such large polarization effects will occur along the b and c axes. A large induced dipole moment $\Delta\mu_a$ was also observed in benzene · SO_2.[7] Confirmation of the structure from fit I as the preferred one, can also be seen by comparing the substitution and the calculated b and c coordinates. The structure from the preferred fit is shown in Fig. 3. The equilibrium orientation of the methyl group about the C_3 axis in this figure is arbitrary since it cannot be determined from the isotopic species studied. The principal axis coordinates for the preferred structure are listed in Table IX.

IV. DISCUSSION

Previous studies in this lab of other π-type complexes such as ethylene · SO_2,[24] acetylene · SO_2,[25] furan · SO_2,[18] and benzene · SO_2 (Ref. 7) have shown that the electrostatic interaction model of Buckingham and Fowler[26] can rationalize conformational features. This approach places distributed multipole moments at atom sites and employs a hard sphere repulsive term to calculate the electrostatic interaction energy. For example, the tilt angle of SO_2 was predicted quite well in the complexes with C_2H_2, C_2H_4, and C_6H_6, and insights on the asymmetric structure in furan · SO_2 were obtained. In the remainder of this section we will explore the applicability of this model to toluene · SO_2.

The distributed multipole values for SO_2 were taken from Ref. 26. Those for toluene were calculated using the distributed multipole analysis (DMA) (Ref. 27) sections of the CADPAC program.[28] The distributed multipole values for toluene are listed in Table X. The structure of toluene employed in the calculation of the multipoles is taken from Ref. 17, where the orientation of the methyl group is arbitrarily chosen, such that the C–H′ bond is perpendicular to the aromatic ring. It should be noted that slightly different values for the distributed multipoles are obtained for other orientations of the methyl group. The effect of this variation on conclusions will be noted in several places subsequently.

In view of the crudeness of the model, especially the repulsive term, a global energy minimization was not attempted. However, the energy changes were explored as some of the structural parameters were varied from their observed values to learn if the electrostatic model (ESM) appeared to predict conformational features close to the observed. Just as in the case of benzene · SO_2, the ESM prefers a SO_2 orientation with the sulfur end closer to the aromatic ring, and the calculated tilt angle, θ_1, was consistent with the observed value. An additional and somewhat unexpected feature is the structural asymmetry in the toluene · SO_2 complex. The C_2 axis of SO_2 is rotated by 47° from the C_3 axis of toluene (see Sec. III C). Interestingly, similar asymmetry was also observed in furan · SO_2.[18] To explore whether the asymmetry in toluene · SO_2 could be attributed to electrostatic interactions, we employed the Buckingham–Fowler model. This model gave a shallow minimum of the energy around $\tau=20°$–$60°$ which is roughly consistent with the experimental structure. In this calculation the five other van der Waals structural parameters were held fixed to their observed values (configuration I in Table VII).

TABLE IX. Principal axis coordinates (in Å) from configuration I of $C_7H_8 \cdot SO_2$.

Atom[a]	a	b	c
C_1	1.305	0.954	0.240
C_2	1.090	0.047	1.281
C_3	1.196	−1.327	1.069
C_4	1.522	−1.816	−0.199
C_5	1.740	−0.917	−1.247
C_6	1.631	0.455	−1.024
C_1'	1.189	2.441	0.477
H_2	0.836	0.401	2.274
H_3	1.023	−2.010	1.896
H_4	1.606	−2.879	−0.368
H_5	1.994	−1.278	−2.239
H_6	1.804	1.131	−1.853
H_1'	2.160	2.864	0.780
H_2'	0.859	2.956	−0.440
H_3'	0.457	2.653	1.273
O_a	−2.007	1.219	−0.443
O_b	−2.440	−0.968	0.621
S	−1.745	−0.185	−0.354

[a]The atoms of the aromatic ring are labeled 1–6 in a clockwise fashion looking from the SO_2 side [see Fig. 3(a)]. C_1 is attached to C_1' of the methyl group. The primed hydrogens belong to methyl, with H_2' and H_3' being on the SO_2 side. O_a is closer to the methyl group.

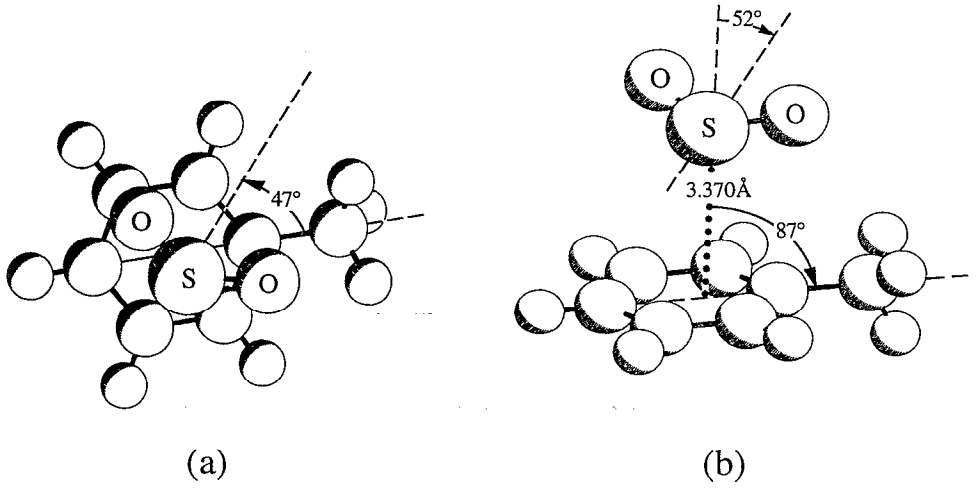

FIG. 3. Molecular structure of toluene · SO_2 from the least-squares fit I. (a) Top view of the complex where SO_2 is placed on top of the aromatic ring. (b) Side view of the complex where the dotted line (R_{cm}) joining the centers of mass of each subunit is nearly aligned with the a axis. The values of the two additional twist angles ϕ_1 and ϕ_2 are not shown (see text).

TABLE X. Cartesian coordinates (in Å) and distributed multipoles (in a.u.) for toluene.[a]

Atom[b]	x	y	z	q	μ_x	μ_y	μ_z	Θ_{xx}	Θ_{yy}	Θ_{zz}	Θ_{xy}	Θ_{xz}	Θ_{yz}
C (1)	0.0	−1.865	0.0	−0.072	0.0	0.022	−0.004	0.215	−0.185	−0.030	0.0	0.0	−0.005
C (2)	−1.207	−1.160	0.0	−0.051	0.026	0.016	−0.004	−0.125	0.112	0.012	−0.180	0.006	−0.015
C (3)	−1.201	0.234	0.0	−0.003	0.192	−0.113	−0.007	0.189	0.028	−0.217	−0.138	−0.027	−0.015
C (4)	0.0	0.948	0.0	−0.019	0.0	0.208	0.031	−0.008	0.143	−0.135	0.0	0.0	−0.036
C (5)	0.0	2.457	0.0	−0.014	0.0	−0.253	0.0	−0.309	0.524	−0.214	0.0	0.0	0.008
H (1)	0.0	−2.945	0.0	0.032	0.0	−0.216	0.0	0.049	−0.086	0.037	0.0	0.0	0.0
H (2)	−2.153	−1.694	0.0	0.035	−0.188	−0.106	0.0	−0.054	0.017	0.038	−0.059	0.0	0.0
H (3)	−2.152	0.753	0.0	0.029	−0.191	0.097	0.001	−0.056	0.016	0.040	0.051	0.002	0.002
H′ (5)	0.0	2.847	1.031	0.019	0.0	0.071	0.186	0.038	0.026	−0.064	0.0	0.0	−0.041
H″ (5)	−0.893	2.847	−0.515	0.017	−0.159	0.074	−0.095	−0.037	0.022	0.015	0.031	−0.043	0.023

[a]The distributed multipoles are calculated at the HF/6-31G** level.
[b]Distributed multipoles for equivalent sites follow by symmetry about the yz plane.

The ESM was also consistent with the fact that configuration I is preferred compared to configuration II (see Sec. III C). The calculated binding energy for conformation I was 2.6–2.8 kcal mol^{-1}, while it was 0.7–0.9 kcal mol^{-1} lower for configuration II. As mentioned above, a range for these binding energies was obtained depending on the methyl orientation. For comparison, using the observed D_J and the modified pseudodiatomic approximation,[29] a value of 2.4 kcal mol^{-1} is calculated for the binding energy. This value is 0.5 kcal mol^{-1} higher than the value calculated similarly for benzene · SO_2. This lends support to the early work on complexes of SO_2 in solution,[1] which deduced that methyl substitution in benzene derivatives enhances the interaction with SO_2. Since the experimental value for the binding energy in benzene · SO_2 has been determined as 4.4(3) kcal mol^{-1},[30] the true value for toluene · SO_2 is likely to be ~5 kcal mol^{-1}.

In the spectral assignment we found that the effects from internal rotation of the methyl group are observable in the toluene · SO_2 complex. The barrier to internal rotation derived from fitting of the torsional-rotational spectrum is V_3=84 cm^{-1}. In free toluene the internal rotation barrier is V_6=4.9 cm^{-1}.[8] Although toluene · SO_2 is a weakly bound complex type, the presence of SO_2 in the vicinity of toluene has a relatively large effect on the methyl internal rotation. In the work on benzene · SO_2,[7] we showed that the observed barrier to internal rotation of benzene about its C_6 axis is in good agreement with that predicted with the Buckingham–Fowler electrostatic model. We also used this model to investigate whether we can mimic the observed barrier in toluene · SO_2. This gave a value of V_3=87.3 cm^{-1} for the barrier to internal rotation of the methyl group. Although this calculated barrier is in striking agreement with the experimental value, a lower value (V_3=26.6 cm^{-1}) was also obtained when a second set of multipole values was used for toluene. The second set of the distributed multipoles corresponds to a toluene conformation where the C–H′ bond of the methyl group is parallel to the ring plane. This suggests that calculations of the barrier with an electrostatic model must concern itself with the variance in multipole moments with methyl orientations in order to obtain useful results. Nonetheless, it is compelling to note that based on electrostatic interactions, the presence of SO_2 in the vicinity of toluene, increases the V_3 component of the methyl group barrier to values of the right magnitude. Of course, the large polarization of the toluene destroys the symmetry in the π cloud seen by the methyl group in free toluene, and this electronic effect could also contribute to the barrier. It is impossible to separate this electronic effect from a purely electrostatic interaction between the SO_2 and toluene without a more sophisticated theoretical analysis, which is beyond the scope of this study.

In addition to the internal rotation of methyl, evidence of a reorientation tunneling motion of SO_2 relative to the aromatic ring was also observed. This result is similar to that in benzene · SO_2 where nearly free internal rotation of benzene (or conversely SO_2) occurred, in the sense that in both complexes a cooperative internal motion of SO_2 and the aromatic ring is involved. However, unlike in benzene · SO_2 where the internal rotation caused a considerable perturbation on the spectrum,[7] in toluene · SO_2 the tunneling motion was a minor perturbation (see Sec. III A). We used the ESM to map out a potential function for the reorientation motion in toluene · SO_2 which is similar to the internal rotation observed in benzene · SO_2. This is pathway 1→3 in Fig. 1. The potential functions (electrostatic energies) with respect to τ (see definition in Sec. III C) are shown in Fig. 4. Figure 4(a) corresponds to methyl oriented in such a way that two hydrogens are placed on the SO_2 side, and in Fig. 4(b) the methyl is oriented so that one hydrogen is placed on the SO_2 side. In these calculations θ_1, θ_2, and R_{cm} were fixed to their experimental values (see Sec. III C), whereas ϕ_1 and ϕ_2 were fixed to 90°. The first striking result from these two plots is that the shape of the potential function is sensitive to the orientation of the methyl group. The potential function in Fig. 4(a) is not as compatible with the experimental results as the potential function in Fig. 4(b). In the former case the torsion of SO_2 about R_{cm} has to overcome a large barrier ($E_{\tau=180°}-E_{\tau=0°}$=150 cm^{-1}). On the other hand, the potential function in Fig. 4(b), implies that the reorientation tunneling motion is more feasible if it follows the pathway through τ=0° (*para* position) with a barrier height of 61 cm^{-1}. For tunneling in the opposite direction, the maximum occurs at τ=150° with a barrier of 216 cm^{-1}. This

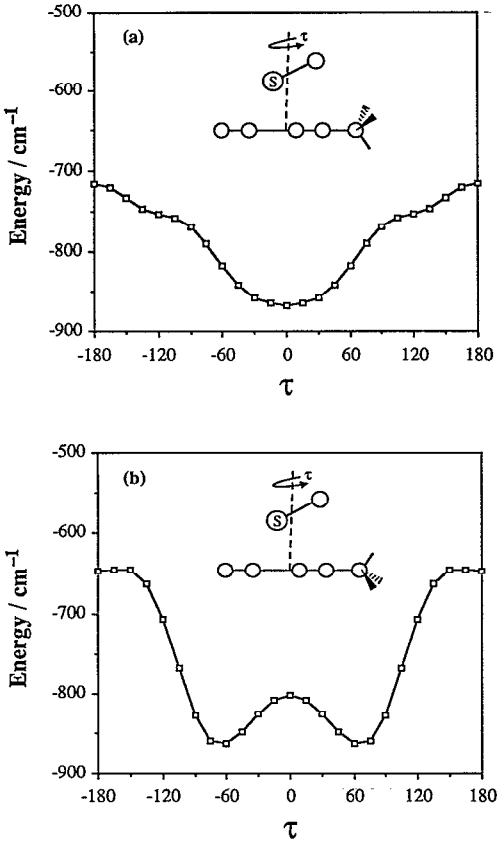

FIG. 4. Electrostatic interaction energy with respect to the torsional angle τ in toluene · SO_2. Plot (a) corresponds to methyl oriented so that two hydrogens are on the SO_2 side. In plot (b) only one hydrogen is on the SO_2 side.

makes a good physical sense, i.e., a lower barrier when the SO_2 avoids "bumping" with the methyl group. It also suggests that the SO_2–toluene reorientation motion and the methyl tunneling may be closely coupled motions. Lastly, it should be noted that, as mentioned in Sec. III A 3, a second pathway (other than a benzene · SO_2-like internal motion) is also possible and cannot be precluded based on the available experimental data. An ESM estimation of the barrier height was not attempted since a more complicated pathway is involved.

In summary, a wealth of information has been garnered about the toluene · SO_2 complex ranging from an interesting structural asymmetry, polarization effects, and internal dynamics. This is indeed an appealing system to obtain complementary insights from more sophisticated electrostatic or *ab initio* calculations, which we hope will be forthcoming in due course.

ACKNOWLEDGMENTS

The work was supported by the Experimental Physical Chemistry Program, National Science Foundation, Washington, D.C. The authors are grateful to the Donors of the Petroleum Research Fund, American Chemical Society for the support of this work in the form of fellowship stipends to A. T.-B. An allotment of computing time for calculations at the San Diego Supercomputer center is gratefully acknowledged.

[1] L. J. Andrews and R. M. Keefer, J. Am. Chem. Soc. **73**, 4169 (1951).
[2] P. A. D. de Maine, J. Chem. Phys. **26**, 1036 (1957).
[3] D. Booth, F. S. Dainton, and K. J. Ivin, Trans. Faraday Soc. **55**, 1293 (1959).
[4] B. C. Smith and G. H. Smith, J. Chem. Soc. **1965**, 5514.
[5] B. S. Ault, J. Mol. Struct. **238**, 111 (1990).
[6] M. S. LaBarge, J. J. Oh, K. W. Hillig II, and R. L. Kuczkowski, Chem. Phys. Lett. **159**, 559 (1989).
[7] A. Taleb-Bendiab, K. W. Hillig II, and R. L. Kuczkowski, J. Chem. Phys. **97**, 2996 (1992).
[8] H. D. Rudolph, H. Dreizler, A. Jaeschke, and P. Wendling, Z. Naturforsch. Teil A **22**, 940 (1967).
[9] K. W. Hillig II, J. Matos, A. Scioly, and R. L. Kuczkowski, Chem. Phys. Lett. **133**, 359 (1987).
[10] R. K. Bohn, K. W. Hillig II, and R. L. Kuczkowski, J. Phys. Chem. **93**, 3456 (1989).
[11] D. Patel, D. Margolese, and T. R. Dyke, J. Chem. Phys. **70**, 2740 (1979).
[12] J. K. G. Watson, *Vibrational Spectra and Structure*, edited by J. R. Durig (Elsevier, Amsterdam, 1977), Vol. 6, Chap. 1.
[13] W. Gordy and R. L. Cook, *Microwave Molecular Spectra* (Wiley, New York, 1984).
[14] D. R. Herschbach, J. Chem. Phys. **31**, 91 (1959).
[15] C. C. Lin and J. D. Swalen, Rev. Mod. Phys. **31**, 841 (1959).
[16] F. Rohart, J. Mol. Spectrosc. **57**, 301 (1975).
[17] V. Amir-Ebrahimi, A. Choplin, J. Demaison, and G. Roussy, J. Mol. Spectrosc. **89**, 42 (1981).
[18] J. J. Oh, L.-W. Xu, A. Taleb-Bendiab, K. W. Hillig II, and R. L. Kuczkowski, J. Mol. Spectrosc. **153**, 497 (1992).
[19] R. W. Kilb, C. C. Lin, and E. B. Wilson, Jr., J. Chem. Phys. **26**, 1695 (1957).
[20] P. A. Helminger and F. C. DeLucia, J. Mol. Spectrosc. **111**, 66 (1985).
[21] W. A. Kreiner, H. D. Rudolph, and B. T. Tan, J. Mol. Spectrosc. **48**, 86 (1973).
[22] M. D. Harmony, V. W. Laurie, R. L. Kuczkowski, R. H. Schwendeman, D. A. Ramsey, F. J. Lovas, W. J. Lafferty, and A. G. Maki, J. Phys. Chem. Ref. Data **8**, 619 (1979).
[23] J. Kraitchman, Am. J. Phys. **21**, 17 (1953).
[24] A. M. Andrews, A. Taleb-Bendiab, M. S. LaBarge, K. W. Hillig II, and R. L. Kuczkowski, J. Chem. Phys. **93**, 7030 (1990).
[25] A. M. Andrews, K. W. Hillig II, R. L. Kuczkowski, A. C. Legon, and N. Howard, J. Chem. Phys. **94**, 6947 (1991).
[26] A. D. Buckingham and P. W. Fowler, Can. J. Chem. **63**, 2018 (1985).
[27] A. J. Stone, Chem. Phys. Lett. **83**, 233 (1981).
[28] R. D. Amos and J. E. Rice, Cambridge Analytical Derivatives Package (CADPAC), issue 4.0, 1987.
[29] D. J. Millen, Can. J. Chem. **63**, 1477 (1985).
[30] J. R. Grover, E. A. Walters, J. K. Newman, and M. G. White, J. Am. Chem. Soc. **107**, 7329 (1985).